ChemComm

Construction of ligand-binding controlled hemoprotein assemblies utilizing 3D domain swapping

Journal:	*ChemComm*
Manuscript ID	CC-COM-06-2024-003129.R1
Article Type:	Communication

COMMUNICATION

Construction of ligand-binding controlled hemoprotein assemblies utilizing 3D domain swapping

Received 00th January 20xx,
Accepted 00th January 20xx

DOI: 10.1039/x0xx00000x

Tsuyoshi Mashima,*[a] Masaru Yamanaka,[a] Atsuki Yoshida,[a] Naoya Kobayashi,[a] Yui Kanaoka,[b] Takayuki Uchihashi[b, c] and Shun Hirota*[a]

Association-controllable hemoprotein assemblies were constructed from a fusion protein containing two *c*-type cytochrome units, using 3D domain swapping. The hemoprotein assembly exhibited a dynamic exchange between cyclic and linear structures and could be regulated by carbon monoxide (CO) and imidazole binding.

In nature, protein assemblies play an important role in biomolecule production, storage, and transfer.[1] These protein assembly functions are frequently regulated by structural changes induced by small molecules.[2,3] Accordingly, protein assemblies have been constructed as new functional biomaterials[4-7] that exhibit various structures, including rings[8-10], 2D sheets[11-13], tubes[14-17], and cages.[4,18-20] In particular, studies to control protein assemblies have been performed utilizing metal coordination[12,21], disulfide bond[22], substrate or DNA binding,[23-25] and light-induced structural changes.[26] However, these responses may be relatively slow, whereas binding of small molecule ligands to the protein is effective for rapid control of protein assemblies. Here, we constructed a hemoprotein assembly wherein oligomerization was controlled by chemical stimuli, such as carbon monoxide (CO) and imidazole binding. The designed unit of this protein assembly was based on 3D domain swapping (3D-DS) wherein the same structural region was exchanged three-dimensionally between molecules of the same protein.[27,28]

Hemoproteins possess the hydrophobic iron protoporphyrin IX (heme) as a cofactor that plays a key role in their functions. In the 3D-DS of hemoproteins, heme serves as a large hydrophobic layer between domains and stabilises the 3D-DS structure. In particular, 3D-DS is frequently obtained in *c*-type heme proteins because the heme is attached to the polypeptide via covalent bonds and does not dissociate during 3D-DS oligomerization.[29-31] *Allochromatium vinosum* cytochrome *c'* (AVCP) is a gas-binding *c*-type cytochrome that exhibits a unique reversible monomer–dimer transition based on CO binding to heme iron (Fig. 1a).[32-35] The dissociation of the dimer to monomers in AVCP has been attributed to the displacement of Tyr16 from the distal site of heme upon CO binding, which results in a conformational change in one of the α-helices at the dimer interface. A tetramer comprising one 3D-DS dimer and two AVCP monomers dissociated into a 3D-DS dimer and two monomers in the presence of CO.[36] Meanwhile, we constructed a circular permutated protein (CPC) from hyperthermostable

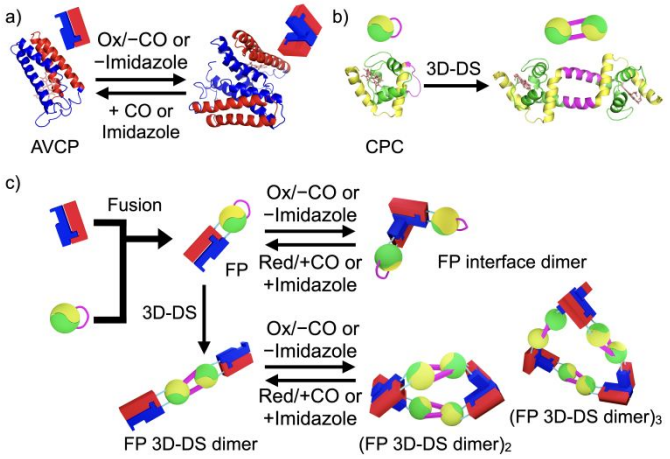

Figure 1. a) Schematic representation of monomer-dimer equilibrium of AVCP (PDB ID: 1BBH) controlled by CO binding. N- and C-terminal regions are depicted in blue and red, respectively. Hemes are shown in pink. b) Schematic representation of CPC 3D-DS dimerization. The monomer and dimer structures of CPC are predicted with AlphaFold2 using one and two molecules, respectively. The N-terminal region, C-terminal region, and inserted linker are shown in green, yellow, and magenta, respectively. Hemes are shown in pink. c) Schematic representation of FP constructed by fusion of AVCP and CPC,

[a] *Division of Materials Science, Graduate School of Science and Technology, Nara Institute of Science and Technology, 8916-5 Takayama, Ikoma, Nara 630-0192, Japan.*
E-mail: t.mashima@ms.naist.jp, hirota@ms.naist.jp
[b] *Department of Physics, Nagoya University, Nagoya, 464-8602, Japan.*
[c] *Exploratory Research Center on Life and Living Systems (ExCELLS), National Institutes of Natural Sciences, Higashiyama 5-1, Myodaiji, Okazaki, 444–0864 Japan*
† Electronic Supplementary Information (ESI) available. See DOI: 10.1039/x0xx00000x

monomer-dimer equilibrium of FP, 3D-DS dimerization of FP, and oligomerization control of FP 3D-DS dimer by CO binding.

Aquifexaeolicus cytochrome c_{555} by inducing intermolecular interactions through insertion of an α-helical linker between the original N- and C-terminal α-helices. CPC was obtained as a monomer from engineered *Escherichia* (*E.*) *coli*. CPC effectively formed dimers, trimers, and oligomers by the procedure of ethanol addition, lyophilisation, and residual redissolution (Fig. 1b),[37] like the 3D-DS oligomerization procedure of other hemoproteins.[27,28] In this study, a fusion protein (FP) of AVCP and CPC was constructed by splitting AVCP in the middle of the protein and connecting the C-terminal half of AVCP to the N-terminus of CPC, and the N-terminal half of AVCP to the C-terminus of CPC (Fig. 1c). FP dimerised and presumably formed a 3D-DS dimer upon ethanol addition, lyophilisation, and residual redissolution. The FP 3D-DS dimer further oligomerized via intermolecular interactions between the AVCP domains, constructing protein assemblies.

FP was expressed in *E. coli* possessing a cytochrome *c* maturation system and was obtained in a dimeric state (FP interface dimer, Fig. 1C and Fig. S2, ESI†), facilitating easy purification. The preserved dimerization interface of the AVCP structural unit in FP may interact intermolecularly to produce the interface dimer. After oxidation with potassium ferricyanide, the FP interface dimer was purified by ion exchange and size-exclusion chromatography (SEC). The purity of FP was confirmed by SDS-PAGE (Fig. S1, ESI†). The UV-vis spectrum of the FP interface dimer corresponded well to the sum of the AVCP and CPC spectra, suggesting that the structures around the hemes of the AVCP and CPC structural units of FP maintained the corresponding structures of the original AVCP and CPC (Fig. 2a). The circular dichroism (CD) spectrum of the FP interface dimer also corresponded with the sum of the AVCP and CPC spectra (Fig. S3a, ESI†). These results indicated that no significant structural changes occurred in the AVCP and CPC structural units of the FP upon fusion.

The UV-vis spectrum of the FP interface dimer exhibited similar changes to the AVCP spectrum upon CO binding to reduced heme (Fig. S4, ESI†), indicating the preserved CO-binding ability of the AVCP structural unit in FP. The FP interface dimer dissociated into monomers by CO binding through dithionite addition under a CO atmosphere (Fig. 2b), similar to AVCP.[32-34] According to the changes in the UV-vis spectra (Fig. S5a, ESI†), imidazole bound to the oxidised heme of FP in air, causing the FP dimer to dissociate into monomers (Fig. S6, ESI†). Imidazole may coordinate to the heme iron of the AVCP unit as the sixth ligand, weakening the interactions between AVCP structural units and leading to the dissociation of the FP interface dimer to monomers. These results supported the hypothesis that FP dimerises through interactions between AVCP structural units and maintains its response to CO and imidazole as AVCP. According to the temperature-dependent CD ellipticity measurement at 222 nm (Fig. S3b, ESI†), the thermal denaturation temperature of the FP interface dimer was 5.6 °C lower than that of the AVCP dimer, indicating a slight decrease in the stability of the FP interface dimer compared to that of AVCP. AVCP and CPC were positively charged on average, which may result in repulsion within FP and contribute to a slight destabilisation.

The FP interface dimer was treated with ethanol and lyophilised, and the residue was redissolved in buffer to obtain the 3D-DS dimer (FP 3D-DS dimer). The optimal ethanol concentration to obtain the FP 3D-DS dimer was 40% (v/v) (Fig. 2c and Fig. S7, ESI†). The FP 3D-DS dimer was stable in the presence of dithionite under a CO atmosphere and was isolated by SEC with a buffer containing dithionite under a CO atmosphere. These results supported the hypothesis that the FP 3D-DS dimer was dimerised by 3D-DS rather than intermolecular interactions between AVCP structural units. The estimated molecular weight of the FP 3D-DS dimer obtained by SEC-multi angle light scattering (SEC-MALS) measurement was 47.1 kDa, which was close to the calculated value, 50.6 kDa (Fig. 2c). The UV-vis spectra of the FP 3D-DS dimer under air and CO atmospheres after reduction were almost identical to the corresponding spectra of FP (Fig. S8 and S9, ESI†), indicating that the structure around the heme and the CO-binding ability of FP were not lost after 3D-DS dimerization. The spectrum of the FP 3D-DS dimer changed upon imidazole addition (Fig. S10, ESI†), and the binding constant K_a (16.6 mM^{-1}) calculated from the changes of the Soret peak by imidazole titration was close to that of FP (K_a = 10.0 mM^{-1}) (Fig. S5b, ESI†), indicating that the structure around the heme was preserved after 3D-DS

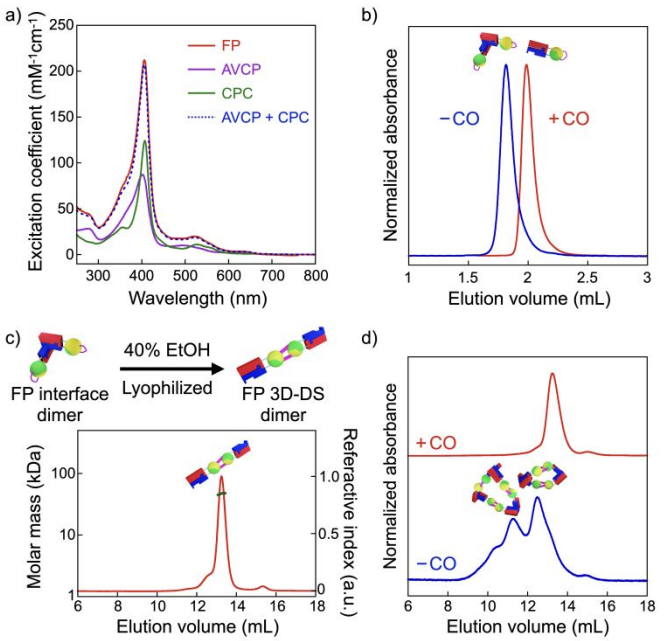

Figure 2. a) UV-vis spectra of FP (red), AVCP (purple), and CPC (green) in 50 mM potassium phosphate buffer, pH 7.0 at 20 °C, and the sum spectrum of AVCP and CPC spectra (blue, dotted). b) SEC traces of 150 μM FP using a Superdex 200 Increase 5/150 column eluted with 50 mM potassium phosphate buffer, pH 7.0 (blue), and the same buffer containing 5 mM dithionite bubbled with CO (red) at 4 °C. Schematic representations of the FP monomer and dimer are shown. c) Schematic representation of 3D-DS dimerization of FP and SEC-MALS analysis of the FP 3D-DS dimer in 50 mM potassium phosphate buffer, pH 7.0, containing 10 mM imidazole at room temperature using a Superdex 200 Increase 10/300 column. d) SEC traces of the FP 3D-DS dimer using

a Superdex 200 Increase 10/300 column eluted with 50 mM potassium phosphate buffer, pH 7.0 (blue), and the same buffer containing 5 mM dithionite bubbled with CO (red) at 4 °C. The FP 3D-DS dimer concentration was 5 μM in monomer unit. Schematic representations of (FP 3D-DS dimer)$_2$ and (FP 3D-DS dimer)$_3$ are shown. Monitoring wavelength was 410 nm for all SEC measurements.

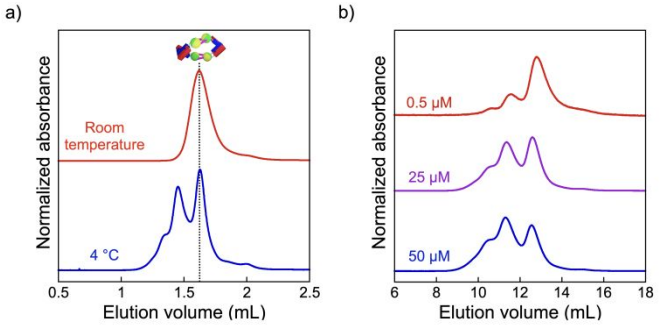

Figure 3. a) SEC traces of the FP 3D-DS dimer using a Superdex 200 Increase 5/150 column eluted with 50 mM potassium phosphate buffer, pH 7.0, at room temperature (red) and 4 °C (blue). The monitoring wavelength was 410 nm. The FP 3D-DS dimer concentration was 25 μM in monomer unit. A schematic representation of (FP 3D-DS dimer)$_2$ is shown. b) SEC traces of the FP 3D-DS dimer at various protein concentrations using a Superdex 200 Increase 10/300 column eluted with 50 mM potassium phosphate buffer, pH 7.0, at 4 °C. The FP 3D-DS dimer concentrations were 0.5 (red), 25 (purple), and 50 μM (blue) in monomer unit. The monitoring wavelength was 410 nm.

dimerization. Interestingly, the FP 3D-DS dimer further oligomerized, forming tetramers (dimers of FP 3D-DS dimers; (FP 3D-DS dimer)$_2$), hexamers (trimers of FP 3D-DS dimers; (FP 3D-DS dimer)$_3$) and higher-order oligomers in air, and dissociated to 3D-DS dimers upon imidazole addition (Fig. 2d and Fig. S11, ESI†). The constructed oligomers were also dissociated into FP 3D-DS dimers by adding dithionite under a CO atmosphere (Fig. S12, ESI†), demonstrating that ligand-binding-controlled protein assemblies were formed with FP 3D-DS dimers. Oligomerization of the FP 3D-DS dimer depended on the temperature and protein concentration. The affinity between AVCP structural units of the FP 3D-DS dimer varied with the temperature. At room temperature, (FP 3D-DS dimer)$_2$ was relatively stable, whereas the FP 3D-DS dimer was associated in (FP 3D-DS dimer)$_3$ and higher-order oligomers (Fig. 3a). Additionally, the ratio of (FP 3D-DS dimer)$_2$, (FP 3D-DS dimer)$_3$, and higher-order oligomers of the FP 3D-DS dimer dramatically changed with protein concentration at 4 °C (Fig. 3b). (FP 3D-DS dimer)$_2$ was mainly detected at 0.5 μM protein concentration, while mainly (FP 3D-DS dimer)$_3$ and higher-order oligomers were observed at higher concentrations, such as 25 and 50 μM. These results indicated that the assemblies of the FP 3D-DS dimers were dynamic. The structure of (FP 3D-DS dimer)$_2$ was observed by high-speed atomic force microscopy (AFM) on a mica substrate at a very low dimer concentration (25 nM) at room temperature (Fig. S13, ESI†). Ring-shaped images with diameters of approximately 20 nm were obtained (Fig. 4a). These structures matched well with the simulated structure calculated from the AlphaFold2-predicted structure of (FP 3D-DS dimer)$_2$ (Fig. 4b and Fig. S14, ESI†). Additionally, a linear structure was observed that matched the other simulated structure of (FP 3D-DS dimer)$_2$, wherein only one AVCP structural unit of the FP 3D-DS dimer interacted intermolecularly (Fig. S15, ESI†). However, the structure of (FP 3D-DS dimer)$_2$ rapidly changed between cyclic and linear structures during the AFM observation (Movie S1, ESI†), suggesting that the ring-shaped structure was dynamic.

In summary, cyclic and linear assemblies of the FP 3D-DS dimer were formed via intermolecular interactions between

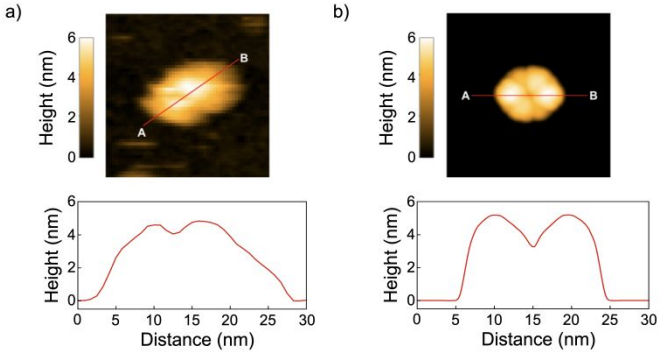

Figure 4. AFM images (top) and sliced heights (bottom) of the ring-shaped (FP 3D-DS dimer)$_2$: a) representative and b) simulated images. The FP 3D-DS dimer concentration was 25 nM in monomer unit.

AVCP structural units of the dimer. The assemblies were controlled by ligand binding, such as CO addition under reducing conditions and imidazole under air. These ligand-binding-controlled protein assemblies could be further fused with other proteins, potentially providing additional functions. The protein assembly system using 3D-DS may serve as a basis for future artificial supramolecular protein assemblies.

This work was financially supported by Grants-in-Aid from JSPS for Scientific Research (B) (No. JP21H02060 (S.H.)) and Scientific Research (C) (No. JP21K04850 (M.Y.)), by JST CREST, Japan (No. JP20338388 (S.H.)), and by KOSÉ Cosmetology Research Foundation (T.M.).

Data availability

The data supporting this article have been included as part of the ESI†.

Conflicts of interest

There are no conflicts to declare.

Notes and references

1 B. J. Pieters, M. B. van Eldijk, R. J. Nolte and J. Mecinovic, *Chem. Soc. Rev.*, 2016, **45**, 24-39.
2 R. P. Bhattacharyya, A. Remenyi, B. J. Yeh and W. A. Lim, *Annu. Rev. Biochem.*, 2006, **75**, 655-680.
3 M. C. Good, J. G. Zalatan and W. A. Lim, *Science*, 2011, **332**, 680-686.
4 Y. T. Lai, G. L. Hura, K. N. Dyer, H. Y. Tang, J. A. Tainer and T. O. Yeates, *Sci. Adv.*, 2016, **2**, e1501855.
5 T. O. Yeates, *Annu. Rev. Biophys.*, 2017, **46**, 23-42.
6 S. van Dun, C. Ottmann, L. G. Milroy and L. Brunsveld, *J. Am. Chem. Soc.*, 2017, **139**, 13960-13968.

7 L. Li and G. Chen, *J. Am. Chem. Soc.*, 2022, **144**, 16232-16251.
8 Q. Li, C. R. So, A. Fegan, V. Cody, M. Sarikaya, D. A. Vallera and C. R. Wagner, *J. Am. Chem. Soc.*, 2010, **132**, 17247-17257.
9 A. J. Simon, Y. Zhou, V. Ramasubramani, J. Glaser, A. Pothukuchy, J. Gollihar, J. C. Gerberich, J. C. Leggere, B. R. Morrow, C. Jung, S. C. Glotzer, D. W. Taylor and A. D. Ellington, *Nat. Chem.*, 2019, **11**, 204-212.
10 K. Oohora, R. Kajihara, N. Fujimaki, T. Uchihashi and T. Hayashi, *Chem. Commun.*, 2019, **55**, 1544-1547.
11 S. Gonen, F. DiMaio, T. Gonen and D. Baker, *Science*, 2015, **348**, 1365-1368.
12 Y. Suzuki, G. Cardone, D. Restrepo, P. D. Zavattieri, T. S. Baker and F. A. Tezcan, *Nature*, 2016, **533**, 369-373.
13 Q. Liu, Y. Zhou, A. Shaukat, Z. Meng, D. Kyllonen, I. Seitz, D. Langerreiter, K. Kuntze, A. Priimagi, L. Zheng and M. A. Kostiainen, *Angew. Chem. Int. Ed.*, 2023, **62**, e202303880.
14 T. Komatsu, X. Qu, H. Ihara, M. Fujihara, H. Azuma and H. Ikeda, *J. Am. Chem. Soc.*, 2011, **133**, 3246-3248.
15 S. Biswas, K. Kinbara, T. Niwa, H. Taguchi, N. Ishii, S. Watanabe, K. Miyata, K. Kataoka and T. Aida, *Nat. Chem.*, 2013, **5**, 613-620.
16 M. Du, K. Zhou, R. Yu, Y. Zhai, G. Chen and Q. Wang, *Nano Lett.*, 2021, **21**, 1749-1757.
17 D. M. Shapiro, G. Mandava, S. E. Yalcin, P. Arranz-Gibert, P. J. Dahl, C. Shipps, Y. Gu, V. Srikanth, A. I. Salazar-Morales, J. P. O'Brien, K. Vanderschuren, D. Vu, V. S. Batista, N. S. Malvankar and F. J. Isaacs, *Nat. Commun.*, 2022, **13**, 829.
18 N. Kobayashi, K. Yanase, T. Sato, S. Unzai, M. H. Hecht and R. Arai, *J. Am. Chem. Soc.*, 2015, **137**, 11285-11293.
19 A. Sciore, M. Su, P. Koldewey, J. D. Eschweiler, K. A. Diffley, B. M. Linhares, B. T. Ruotolo, J. C. Bardwell, G. Skiniotis and E. N. Marsh, *Proc. Natl. Acad. Sci. USA*, 2016, **113**, 8681-8686.
20 N. Ohara, N. Kawakami, R. Arai, N. Adachi, T. Moriya, M. Kawasaki and K. Miyamoto, *J. Am. Chem. Soc.*, 2023, **145**, 216-223.
21 Y. Bai, Q. Luo, W. Zhang, L. Miao, J. Xu, H. Li and J. Liu, *J. Am. Chem. Soc.*, 2013, **135**, 10966-10969.
22 E. R. Ballister, A. H. Lai, R. N. Zuckermann, Y. Cheng and J. D. Mougous, *Proc. Natl. Acad. Sci. USA*, 2008, **105**, 3733-3738.
23 J. M. Karchin, J. H. Ha, K. E. Namitz, M. S. Cosgrove and S. N. Loh, *Sci. Rep.*, 2017, **7**, 44388.
24 J. R. McMillan and C. A. Mirkin, *J. Am. Chem. Soc.*, 2018, **140**, 6776-6779.
25 T. Mashima, B. Rosier, K. Oohora, T. F. A. de Greef, T. Hayashi and L. Brunsveld, *Angew. Chem. Int. Ed.*, 2021, **60**, 11262-11266.
26 J. M. Reis, D. C. Burns and G. A. Woolley, *Biochemistry*, 2014, **53**, 5008-5016.
27 S. Hirota, *J. Inorg. Biochem.*, 2019, **194**, 170-179.
28 S. Hirota, T. Mashima and N. Kobayashi, *Chem. Commun.*, 2021, **57**, 12074-12086.
29 S. Hirota, Y. Hattori, S. Nagao, M. Taketa, H. Komori, H. Kamikubo, Z. Wang, I. Takahashi, S. Negi, Y. Sugiura, M. Kataoka and Y. Higuchi, *Proc. Natl. Acad. Sci. USA*, 2010, **107**, 12854-12859.
30 Y. Hayashi, S. Nagao, H. Osuka, H. Komori, Y. Higuchi and S. Hirota, *Biochemistry*, 2012, **51**, 8608-8616.
31 M. Yamanaka, S. Nagao, H. Komori, Y. Higuchi and S. Hirota, *Protein Sci.*, 2015, **24**, 366-375.
32 M. L. Doyle, S. J. Gill and M. A. Cusanovich, *Biochemistry*, 1986, **25**, 2509-2516.
33 T. H. Evers and M. Merkx, *Biochem. Biophys. Res. Commun.*, 2005, **327**, 668-674.
34 M. A. Hough and C. R. Andrew, *Adv. Microb. Physiol.*, 2015, **67**, 1-84.
35 S. Fujii, M. Masanari, H. Inoue, M. Yamanaka, S. Wakai, H. Nishihara, Y. Sambongi, *Biosci. Biotechnol. Biochem.*, 2013, **77**, 1677-1681.
36 M. Yamanaka, M. Hoshizumi, S. Nagao, R. Nakayama, N. Shibata, Y. Higuchi and S. Hirota, *Protein Sci.*, 2017, **26**, 464-474.
37 A. Oda, S. Nagao, M. Yamanaka, I. Ueda, H. Watanabe, T. Uchihashi, N. Shibata, Y. Higuchi and S. Hirota, *Chem. Asian. J.*, 2018, **13**, 964-967.

Data Availability Statement

June 26, 2024

The data supporting the article titled “Construction of ligand-binding controlled hemoprotein assemblies” have been included as part of the supporting information and supplementally movie.

Shun Hirota

hirota@ms.naist.jp

Graduate School of Science and Technology, Nara Institute of Science and Technology

Tsuyoshi Mashima

t.mashima@ms.naist.jp

Graduate School of Science and Technology, Nara Institute of Science and Technology